Rinkite–nacareniobsite-(Ce) solid solution series and hainite from the Ilímaussaq alkaline complex: occurrence and compositional variation*

JØRN G. RØNSBO, HENNING SØRENSEN†, ENCARNACIÓN RODA-ROBLES, FRANÇOIS FONTAN† & PIERRE MONCHOUX

Rønsbo, J.G., Sørensen, H., Roda-Robles, E., Fontan, F. & Monchoux, P., 2014. Rinkite–nacareniobsite-(Ce) solid solution series and hainite from the Ilímaussaq alkaline complex: occurrence and compositional variation. ©2014 by Bulletin of the Geological Society of Denmark, Vol. 62, pp. 1–15. ISSN 2245-7070. (www.2dgf.dk/publikationer/bulletin). https://doi.org/10.37570/bgsd-2014-62-01

Received 1 August 2013
Accepted in revised form 20 February 2014
Published online 14 March 2014

In the Ilímaussaq alkaline complex, minerals from the rinkite–nacareniobsite-(Ce) solid solution series have been found in pulaskite pegmatite, sodalite foyaite, naujaite and naujaite pegmatite from the roof sequence, and in marginal pegmatite, kakortokite and lujavrite from the floor sequence. The electron microprobe analyses embrace almost the full extension of the solid solution series and confirm its continuity. The solid solution series shows similar compositional variations in the roof and floor sequences: Rinkite members of the series are found in the less evolved rocks in the two sequences, whereas nacareniobsite-Ce members occur in the most evolved rocks and pegmatites in the two sequences. The REE (+Y) content varies from 0.83 atoms per formula unit (apfu) in rinkite from pulaskite pegmatite to 1.31 apfu in nacareniobsite-(Ce) from naujaite pegmatite. The main substitution mechanisms in the solid solution series investigated in this work are $2Ca^{2+} = Na^{+} + REE^{3+}$ and $Ti^{4+} + Ca^{2+} = Nb^{5+} + Na^{+}$. The increased contents of Nb^{5+} and REE^{3+} are only to a minor degree compensated through the $F^{1-} = O^{2-}$ substitution. The chondrite normalised REE patterns of the minerals develop in a similar way in the two sequences, showing relative La-enrichment and Y-depletion from the less to the most evolved rocks.

Hainite has not previously been found in the Ilímaussaq complex. It was here identified in a pulaskite pegmatite sample by a combination of X-ray diffraction giving the unit cell dimensions a = 9.5923(7) Å, b = 7.3505(5) Å, c = 5.7023(4) Å, α = 89.958(2)°, β = 100.260(1)°, γ = 101.100(2)°, and X-ray powder pattern and electron microprobe data giving the empirical formula $(Ca_{1.62}Zr_{0.16}Y_{0.22})(Na_{0.87}Ca_{1.11})(Ca_{1.65}REE_{0.35})Na(Ti_{0.81}Nb_{0.09}Fe_{0.08}Zr_{0.02})(Si_2O_7)_2O_{0.99}F_{2.96}$. Based on published and the present data it is documented that minerals from the hainite-götzenite solid solution series show a compositional variation between the ideal end members $(Y,REE,Zr)Na_2Ca_4Ti(Si_2O_7)_2OF_3$ and $NaCa_6Ti(Si_2O_7)_2OF_3$.

Keywords: Ilímaussaq, rinkite, nacareniobsite-(Ce), hainite, götzenite.

Jørn G. Rønsbo [jornronsbo@gmail.com], Henning Sørensen, Department of Geosciences and Natural Resource Management, University of Copenhagen, Øster Voldgade 10, DK-1350 Copenhagen K, Denmark. Encarnacion Roda-Robles,[encar.roda@ehu.es] Departamento de Mineralogia y Petrologia, Universidad del Pais Vasco/EHU Apdo. 644, E-48080, Bilbao, Spain, François Fontan, Pierre Monchoux, Université de Toulouse, UPS (FSI-OMP), CNRS, IRD-GET, 14 Avenue Edouard Belin, F-31400 Toulouse, France.

* Contribution to the Mineralogy of Ilímaussaq no. 145
† Deceased

Na-bearing disilicates enriched in Ti, Nb, Zr and/or REE (including Y) are typical minerals in agpaitic nepheline syenites both as rock forming minerals and in pegmatites. In the Ilímaussaq alkaline complex, vuonnomite, lomonosovite, murmanite, hiortdahlite, rosenbuschite, epistolite, rinkite and nacareniobsite-(Ce) are present (Petersen 2001). The complex is the type locality for the latter three minerals.

Rinkite and nacareniobsite-(Ce) belong to the rinkite group of minerals together with mosandrite, whereas the other mineral pair of interest in this work, hainite and götzenite, belong to the rosenbuschite

group together with rosenbuschite, seidozerite, kochite and grenmarite. Based on the structural topology, Sokolova (2006) defined four groups of titanium disilicates where the rinkite and rosenbuschite groups belong to the same group (Group I). In this paper we will refer to the traditionally used classification, and when referring to structural sites we use the following general formula for both mineral groups: $M(1)_2M(2)_2M(3)_2M(4)M(5)(Si_2O_7)_2F_2X_2$.

The present study is a paragenetic and mineral chemical investigation of rinkite, nacareniobsite-(Ce) and hainite. The aim of the study is to document the compositional variations in the rinkite–nacareniobsite-(Ce) solid solution series, which has never been investigated, neither in the Ilímaussaq alkaline complex nor elsewhere. During the study a rosenbuschite-group mineral was discovered with the chemical composition of hainite which has not previously been identified in the Ilímaussaq complex.

Geological setting

The Ilímaussaq alkaline complex belongs to the late Precambrian Gardar province of South Greenland (e.g. Upton 2013). The most differentiated and undersaturated rocks in the province are found in this complex, which is characterised by extreme enrichment in incompatible elements including Nb, Zr, REE and F. The basic description of the complex was given by Ussing (1912). Discussions of the petrology and geochemistry of the complex are presented by Larsen & Sørensen (1987), Sørensen & Larsen (1987), Bailey *et al*. (2001), Marks & Markl (2001) and Sørensen (2006). Geological and geochemical evidence indicates that the complex was emplaced in several pulses leading to the formation of an incomplete augite syenite shell, followed by acid peralkaline sheets in the top of the intrusion and finally, a volumetrically dominant sequence of layered perakaline nepheline syenites.

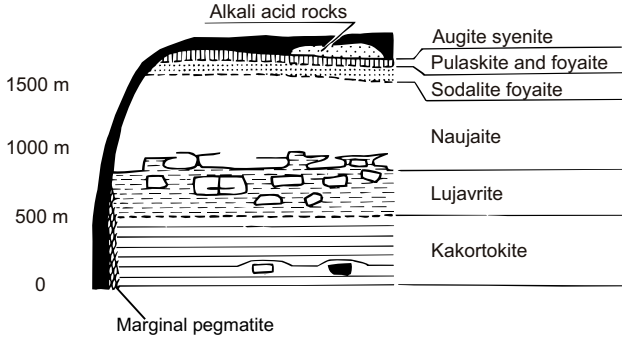

Fig. 1. Diagrammatic E–W section of the southern part of the Ilímaussaq alkaline complex (modified after Andersen *et al.* 1981).

According to one model, the main pulse of peralkaline silica-undersaturated magma led to the formation of the main layered sequence of cumulitic nepheline syenites consisting of a roof sequence, a floor sequence, and an intermediate horizon between the roof and the floor zones. Sørensen (2006) suggested that the floor sequence and the intermediate horizon were formed by a separate magma pulse. In all models, the roof sequence (pulaskite, foyaite, sodalite foyaite and naujaite) crystallized successively downwards from a single magma which became progressively more differentiated. Following Sørensen (2006), a later magma pulse intruded the consolidated roof sequence and formed the floor cumulates (kakortokite) and the intermediate horizon (lujavrite), and it is suggested that the marginal pegmatite represents the early stage of evolution of this melt (Fig. 1). The floor cumulates consist of a layered sequence of kakortokites made of tripartite units, with each unit composed of a lower black layer rich in arfvedsonite which grades upward into a red facies rich in eudialyte which again grades upward into a white facies rich in alkali feldspar. The kakortokites grade upwards into the intermediate horizon which is made up of various types of lujavritic rocks. Moreover, lujavrites also intrude and engulf the overlying roof sequence and locally penetrate into volcanic rocks in the roof, as is the case in the Kvanefjeld area in the northern part of the complex (Sørensen *et al*. 2011). In this work, for the sake of clarity of presentation, we treat the marginal pegmatite, kakortokite and lujavrite together as the 'floor sequence'.

Mineralogy of rinkite, nacareniobsite-(Ce), hainite and götzenite

Rinkite and nacareniobsite-(Ce)

Rinkite, $Na_2Ca_4REETi(Si_2O_7)_2OF_3$, was first described by Lorenzen (1884) based on material collected by K.J.V. Steenstrup in the years 1874, 1876 and 1877 in the Kangerluarsuk area of the Ilímaussaq complex. The type material is kept in the Natural History Museum of Denmark, University of Copenhagen, unfortunately without any information about the exact locality. The crystal structure of rinkite was established by Galli and Alberti (1971).

Some authors, including Fleischer (1958, 1987) and Sokolova & Cámara (2008), argued that rinkite is identical to mosandrite, originally described from nepheline syenite pegmatites in Langesund Fjord, Norway, by Erdmann (1841) and reinvestigated by Brøgger (1890). Johnstrupite (Brøgger 1890) from Langesund, Norway,

and rinkolite and lovchorrite (Bohnstedt 1926) from Khibina, Russia, have also been described as minerals related to rinkite or used as synonyms. Fleischer (1958, 1987) suggested the use of mosandrite in favour of rinkite, rinkolite, lovchorrite and johnstrupite, whereas Slepnev (1957) considered mosandrite to represent an intensively Na- and Ca-leached product of minerals such as rinkite, johnstrupite and rinkolite. Petersen *et al.* (1989) confirmed the existence of a Na- and Ca-leaching process in the niobian rinkite analogue nacareniobsite-(Ce) and further documented that mosandrite crystals from the type locality consist of a Na-Ca-poor fine-grained intergrowth of two minerals. The johnstrupite sample from Barkevik, Langesund (Brøgger 1890) is identical to rinkite (Bellezza *et al.* 2009a).

Recent crystal chemical investigation of mosandrite crystals from the type locality in Langesund, Norway, by Sokolova & Cámara (2008) and Bellezza *et al.* (2009b) led to different results and conclusions. Sokolova & Cámara (2008) concluded that the crystal structure of the museum specimen labelled as mosandrite is chemically and topologically identical to rinkite from the Ilímaussaq alkaline complex. However, they later corrected their statement (Cámara *et al.* 2011) and concluded that the investigated crystal was not mosandrite but rinkite, in agreement with Bellezza *et al.* (2009b) who concluded that mosandrite, $Ti(\square,Ca,Na)_3(Ca,REE)_4(Si_2O_7)_2[H_2O,OH,F]_4 \sim 1H_2O$, is a unique mineral species of the rinkite group and differs from rinkite in chemical composition, with low Ca, Na and F contents and a high amount of H_2O.

Cámara *et al.* (2011) studied the crystal structure of four mineral samples from different localities: Kangerluarsuk, Ilímaussaq, Greenland; Mont Saint-Hilaire, Canada; and two in the Khibina Massif, Russia. They concluded that the four investigated specimens are rinkite and defined rinkite as a valid mineral species with the ideal formula $Na_2Ca_4REETi(Si_2O_7)_2OF_3$. They further suggested a formal redefinition of mosandrite as a valid mineral species. The latest IMA (International Mineralogical Association) official List of Mineral Names (October 2013) includes both mosandrite and rinkite as redefined valid species.

Nacareniobsite-(Ce), $Na_3Ca_3REENb(Si_2O_7)_2OF_3$, was described by Petersen *et al.* (1989) from lujavrite in the Kvanefjeld area of the Ilímaussaq complex and suggested to be a Nb-rich rinkite analogue related by the substitution $Nb^{5+} + Na^{+} = Ti^{4+} + Ca^{2+}$. The crystal structure determination by Sokolova & Hawthorne (2008) confirmed this conclusion.

Table 1. X-ray powder patterns of hainite and götzenite

1		2		3	
d-obs	I	d-obs	I	d-obs	I
		5.57	5	5.640	10
				5.220	10
4.295	10	4.29	5	4.370	10
3.961	50	3.90	10	3.970	20
3.557	10	3.59	5	3.610	10
3.340	10				
3.259	10	3.27	10	3.290	20
3.073	90	3.07	80	3.090	90
2.961	100	2.97	100	2.980	100
2.824	30	2.81	10	2.850	10
2.628	50	2.61	20	2.640	30
2.493	50	2.49	10	2.500	50
2.309	10	2.30	5	2.310	10
2.244	20	2.24	5	2.250	20
2.200	30	2.19	5	2.210	20
				2.120	10
2.043	20	2.04	5	2.060	10
1.984	20			1.991	10
1.896	70	1.90	30	1.913	80
1.865	30			1.871	20
1.822	50	1.83	10	1.833	70
1.787	10	1.79	5	1.797	20

1. Hainite, Johan & Cech 1989. 2 Hainite, Ilímaussaq alkaline complex sample 104029 , Debye Scherrer camera (360 mm) Toulouse, this paper. 3. Götzenite, Sharygin *et al.* 1996.

Hainite and götzenite

In a pegmatite in the uppermost part of the pulaskite in the Ilímaussaq complex, Semenov (1969) found a mineral which is low in REE and high in Ca compared to rinkite, and named it Ca-rinkolite. The sample described by Semenov, and specimens collected by the authors, are included in the present study. Our X-ray diffraction data (Table 1) show that the mineral belongs to the rosenbuschite group of Na, Ti and Zr disilicates and is a member of the götzenite–hainite solid solution series.

Götzenite was first described by Sahama & Hytönen (1957) from nephelinite, Mt. Shareru, Zaire, and the chemical data given by Sahama & Hytönen (1957) are REE- and Zr-free but the high Al content indicates a considerable amount of mineral impurities. The crystal structure was determined by Canillo *et al.* (1972). A götzenite sample from Pian di Celli (Sharygin *et al.* 1996) is low in Zr and REE and approaches the ideal composition $NaCa_6Ti(Si_2O_7)_2OF_3$. Zirconium- and/or REE-bearing götzenite is reported by Sharygin *et al.* (1996), Christiansen *et al.* (2003) and Bellezza *et al.* (2004). The crystal structural data show that Zr can substitute for Ca in the M(1) site (Christiansen *et al.* 2003, Bellezza *et al.* 2004) and for Ti in the M(5) site (Christiansen *et al.* 2003), and the REE substitute for Ca in the M(1) and M(3) sites (Atencio *et al.* 1999, Christiansen *et al.* 2003).

Hainite was first described by Blumrich (1893) in phonolites from Hradiste, Bohemia. A reinvestigation of the type material by Johan and Cech (1989) included microprobe analyses and X-ray powder diffraction data, and they concluded that hainite is isostructural with götzenite but is different in having the (Ca+Na)/(Ti+Zr+Nb) ratio equal to 4, whereas this ratio is 7 in götzenite and 3 in rosenbuschite. Hainite is also described from the Pocos de Caldas alkaline complex, Minas Gerais, by Rastsvetaeva *et al.* (1995) and Atencio *et al.* (1999). According to Rastsvetaeva *et al.* (1995), Ca and Na in hainite are ordered in two independent M(2) sites, leading to space group P1, whereas they are randomly distributed in götzenite, space group $P\bar{1}$ (Canillo *et al.* 1972). Christiansen *et al.* (2003) did not observe any ordering in the M(2) site in hainite from Langesund and reported space group $P\bar{1}$. The same result was obtained by Giester *et al.* (2005) by a crystal structural investigation of hainite from Hradiste. Christiansen *et al.* (2003) observed a small excess Na over Ca in the M(2) site for the sample from Langesund and concluded that "the overall Na/Ca value of this specimen corresponds to that of hainite (Johan & Cech 1989) and we therefore consider the sample as hainite". Based on the crystal structural determination of hainite published by Rastsvetaeva *et al.* (1995), Atencio *et al.* (1999) suggested the simplified formula for hainite to be $Na_2Ca_5Ti(Si_2O_7)_2(OH)_2F_2$.

Electron microprobe analysis and formula calculation

The major part of the electron microprobe analyses presented in this paper were performed on a JEOL 733 Superprobe at the Department of Geosciences and Natural Resource Management, University of Copenhagen. Analytical conditions were 15 nA beam current, 5 microns beam size, and 15 kV acceleration potential except for F which was analysed at 10 kV in order to reduce possible F migration under the electron beam. This was based on analyses of the rinkite type material for F at 8 kV giving 7.7±0.3 wt.% F, at 10 kV giving 7.8±0.3 wt.% F, at 12 kV giving 7.8±0.3 wt.% F, and at 15 kV giving 7.2±0.2 wt.% F. The following X-ray lines and standards were used: FKα: apatite, NaKα: albite, SiKα and CaKα: wollastonite, FeKα: haematite, TiKα: TiO_2, ZrLα: baddeleyite, NbLα: columbite, LaLα: synthetic glass containing 15 wt% La_2O_3, CeLα: CeO_2, PrLβ: $Pr_3Ga_5O_{12}$, NdLα: $Nd_3Ga_5O_{12}$, SmLα: $SmFeO_3$, YLα: $Y_3Al_5O_{15}$. The accuracy of the REE analyses are discussed in Rønsbo (1989).

Of the analyses used here, those from sample 104024, 104034 and 104038 were performed on a Camebax SX50 at Laboratoire de Minéralogie, Université Poul Sabatier, Toulouse. These results have been calibrated towards internal standards to give results comparable to the data obtained in Copenhagen.

The empirical formulae were calculated on the basis of 4 Si in accordance to the structural refinements of the rinkite and rosenbuschite group minerals which show the tetrahedral position to be fully occupied by silicon (Christiansen *et al.* 2003; Belezza *et al.* 2004; Sokolova & Cámara 2008; Sokolova & Hawthorne 2008; Bellezza *et al.* 2009b).

All sample numbers are Geological Institute numbers except 154346 which is a GGU number. The accepted analyses are given in a supplementary data file at the web site http://2dgf.dk/publikationer/bulletin/190bull62.html.

Occurrence, zonation and compositional variation of hainite and rinkite–nacareniobsite-(Ce) in the Ilímaussaq complex

Pulaskite pegmatite

The pegmatite forms a lenticular body in a small occurrence of quartz syenite and pulaskite overlying foyaite on the plateau around Point 535 m between the fiords Kangerluarsuk and Tunulliarfik (Steenfelt 1981). The contact relations are obscured by scree, but pulaskite and its pegmatites are most probably intrusive into the quartz syenite.

The pegmatite is composed of large plates of perthitic alkali feldspar with minor clinopyroxene and amphibole. Hainite occurs as prismatic brown grains that may attain a length of more than 5 cm. Semenov (1969) described the mineral from this locality, referred it to the rinkite group and named it Ca-rinkolite. The name was, however, never approved by the IMA. New X-ray powder diffraction data (Table 1) and the unit cell dimensions a = 9.5923(7) Å, b = 7.3505(5) Å, c=5.7023(4) Å, α = 89.958(2)°, β = 100.260(1)°, γ = 101.100(2)° (numbers in parentheses are 1σ for the last digit), established by the single crystal method, show that the mineral belongs to the rosenbuschite group and is either götzenite or hainite.

The mineral was analysed by electron microprobe in three different samples (104029, 104373 and an unnumbered sample donated by E. Semenov). The mean values for the different samples do not differ significantly, and the analysis in Table 2 (no. 1) is the mean of all 56 analyses. This composition is that of hainite rather than götzenite. The formula calculation gave a total number of cations of 11.96 compared to the ideal

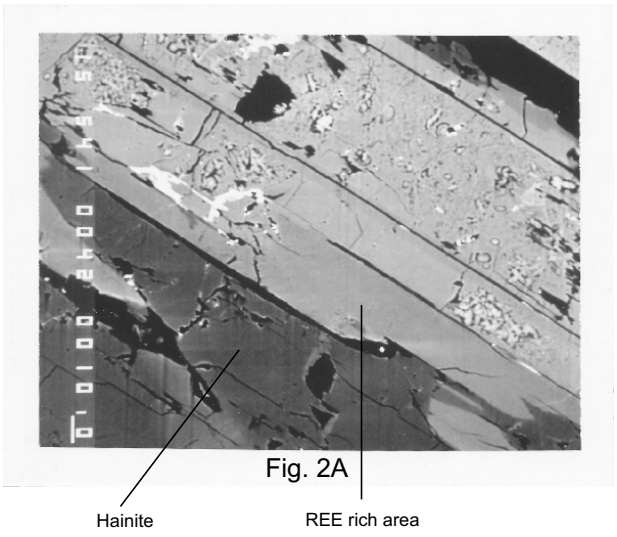

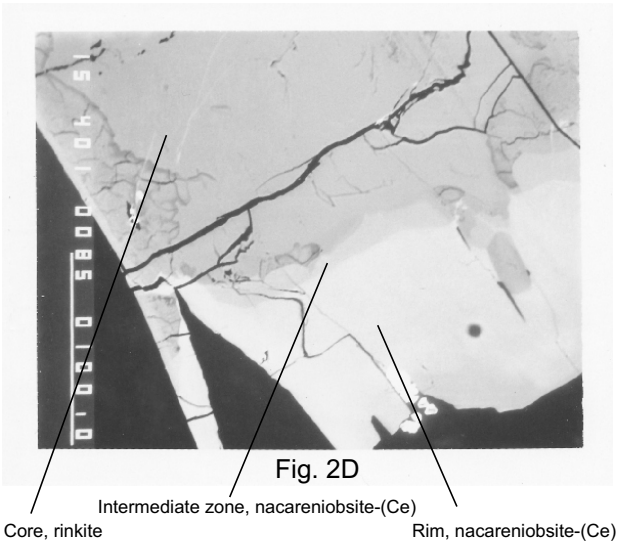

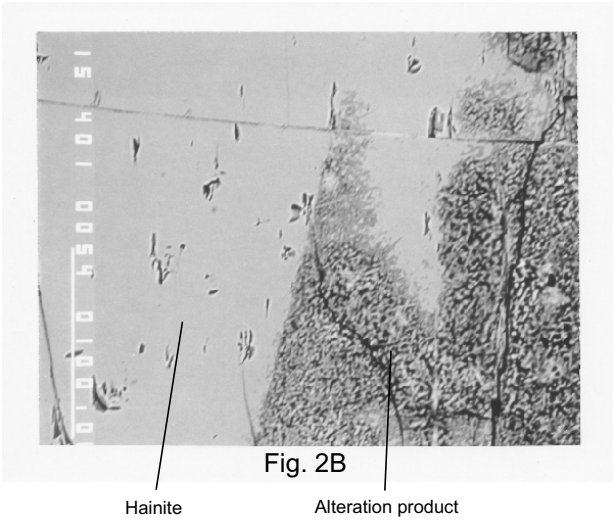

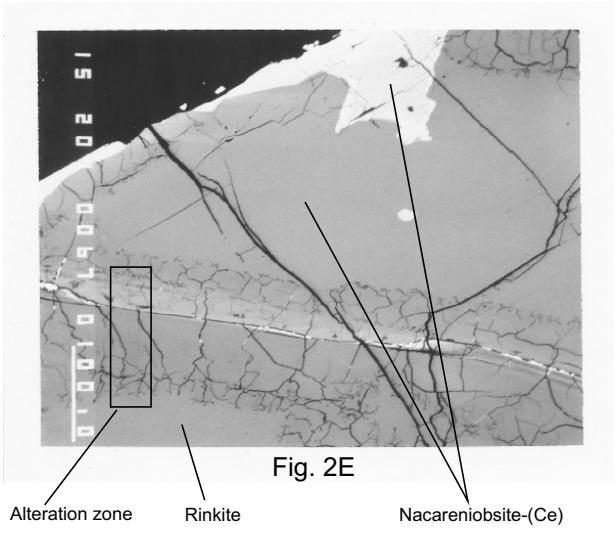

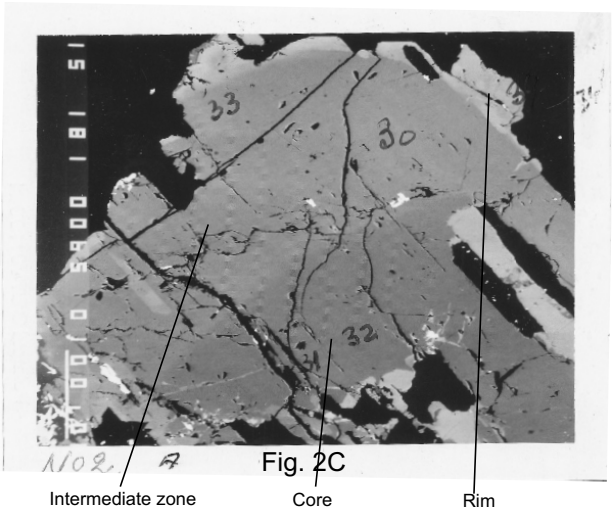

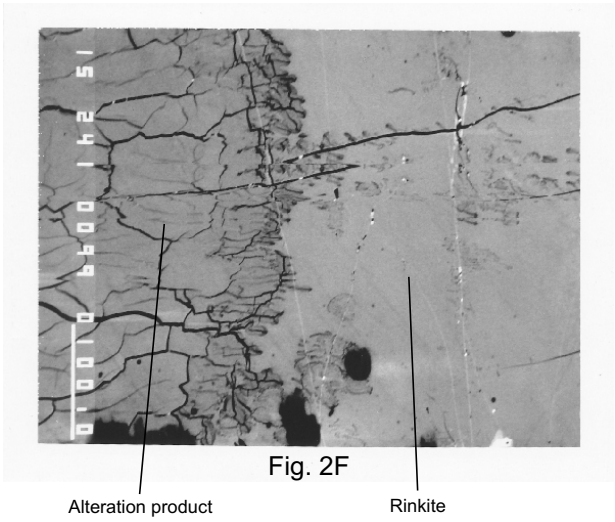

Fig. 2. Backscattered electron images of hainite, rinkite and nacareniobsite-(Ce). **A**, pulaskite pegmatite sample 104029; hainite crystal with REE-enriched area. **B**, Pulaskite pegmatite sample 104373; partly altered hainite. **C**. Sodalite foyaite sample 104375; zoned rinkite. **D**, Naujaite pegmatite sample 104013; zoned rinkite–nacareniobsite-(Ce) crystal. **E**, Naujaite pegmatite sample 104013; zoned rinkite–nacareniobsite-(Ce) crystal with alteration zone. **F**, Naujaite pegmatite sample 104013; partly altered rinkite.

Table 2.

Microprobe analyses of hainite, rinkite and nacareniobsite-(Ce) in pulaskite pegmatite, sodalite foyaite, naujaite and naujaite pegmatite

No.	1	2	3	4	5	6	7	8	9
Rock	Pul.pegmatite	Pul.pegmatite	Pul.pegmatite	Sodal. foyaite	Sodal. foyaite	Sodal. foyaite	Naujaite	Nau.pegmatite	Nau.pegmatite
Sample	Average	104029	104373	104375	104375	104375	104001	104013	104013
Mineral	Hainite	Rinkite	Alteration product	Rinkite	Rinkite	Rinkite	Rinkite	Rinkite	Nacareniobsite-(Ce)
Zone				Core	Mantle	Rim		Core	Core
N	56	3	2	2	2	4	6	5	6
Oxides wt%									
SiO_2	30.65 (.02)	30.02 (.07)	26.80 (.08)	29.67 (.08)	29.57 (.08)	29.09 (.06)	29.64 (.05)	29.00 (.05)	29.38 (.05)
TiO_2	8.23 (.01)	8.91 (.05)	12.74 (.08)	6.17 (.06)	6.28 (.06)	5.28 (.04)	5.64 (.04)	5.43 (.04)	4.32 (.03)
ZrO_2	2.87 (.03)	0.82 (.11)	2.28 (.32)	2.21 (.30)	0.04 (.01)	0.57 (.07)	0.53 (.06)	0.38 (.04)	0.11 (.02)
Nb_2O_5	1.43 (.02)	1.70 (.12)	4.06 (17)	3.28 (.16)	4.62 (.17)	6.28 (.14)	6.55 (.13)	7.12 (.13)	9.35 (.13)
FeO	0.70 (.01)	n.d.	0.66 (.05)	0.20 (.03)	0.08 (.02)	n.d.	n.d.	0.05 (.01)	0.03 (.00)
CaO	31.34 (.02)	28.64 (.10)	19.85 (.10)	26.54 (.09)	24.90 (.11)	22.06 (.07)	23.14 (.06)	23.04 (.06)	22.44 (.06)
Na_2O	7.44 (.02)	7.58 (.07)	3.46 (.09)	7.69 (.07)	8.26 (.08)	9.03 (.06)	9.25 (.06)	9.36 (.06)	9.60 (.05)
La_2O_3	0.95 (.01)	1.65 (.05)	2.23 (.07)	2.33 (.07)	2.87 (.08)	3.08 (.05)	2.92 (.04)	3.89 (.05)	4.67 (.08)
Ce_2O_3	3.14 (.02)	5.36 (.07)	5.88 (.11)	6.65 (.09)	8.22 (.10)	9.36 (.07)	9.12 (.06)	9.86 (.07)	10.02 (.07)
Pr_2O_3	0.45 (.02)	0.86 (.11)	0.65 (.11)	0.81 (.13)	1.04 (.14)	1.24 (.10)	1.07 (.09)	1.00 (.09)	1.01 (.08)
Nd_2O_3	2.06 (.03)	3.60 (.13)	3.41 (.16)	4.02 (.17)	4.56 (.18)	5.12 (.13)	5.04 (.10)	3.85 (.11)	3.42 (.09)
Sm_2O_3	0.34 (.01)	0.66 (.07)	0.70 (.08)	0.74 (.09)	0.69 (.09)	0.92 (.07)	0.81 (.05)	0.52 (.05)	0.44 (.04)
Y_2O_3	3.17 (.01)	3.48 (.05)	5.27 (.06)	2.08 (.07)	1.72 (.07)	1.41 (.05)	2.07 (.04)	1.93 (.05)	1.29 (.04)
F	7.17 (.08)	7.01 (.30)	5.07 (.32)	8.03 (.43)	7.61 (.40)	7.90 (.30)	7.10 (.24)	6.69 (.25)	6.88 (.20)
Total	99.94	100.29	93.06	100.42	100.46	101.34	102.88	102.12	102.96
-O for F	-3.02	-2.95	-2.13	-3.38	-3.20	-3.33	-2.99	-2.82	-2.90
	96.92	97.34	90.93	97.04	97.26	98.01	99.89	99.30	100.06
Cations based on 4 Si									
Si	4.00	4.00	4.00	4.00	4.00	4.00	4.00	4.00	4.00
Ti	0.81	0.89	1.43	0.63	0.64	0.55	0.57	0.56	0.44
Zr	0.18	0.05	0.17	0.15	0.00	0.04	0.03	0.03	0.01
Nb	0.08	0.10	0.27	0.20	0.28	0.39	0.40	0.44	0.58
Fe	0.08	0.00	0.08	0.02	0.01	0.00	0.00	0.01	0.00
Ca	4.38	4.09	3.17	3.83	3.61	3.25	3.35	3.40	3.27
Na	1.88	1.95	1.00	2.01	2.16	2.40	2.42	2.50	2.53
La	0.05	0.08	0.12	0.12	0.14	0.16	0.15	0.20	0.23
Ce	0.15	0.26	0.32	0.33	0.41	0.47	0.45	0.50	0.50
Pr	0.02	0.04	0.04	0.04	0.05	0.06	0.05	0.05	0.05
Nd	0.10	0.17	0.18	0.19	0.22	0.25	0.24	0.19	0.17
Sm	0.01	0.03	0.04	0.03	0.03	0.04	0.04	0.02	0.02
Y	0.22	0.25	0.42	0.15	0.12	0.10	0.15	0.14	0.09
F	2.96	2.95	2.39	3.42	3.26	3.44	3.03	2,92	2.96
Cations	11.96	11.91	11.24	11.70	11.67	11.71	11.85	12.04	11.89
Charges	32.81	32.88	34.61	32.41	32.27	32.45	32.76	33.18	32.95

N: number of analyses. n.d.: not detected. Numbers in parentheses are standard deviations calculated on the basis of the total counting time and count rates on peak and background and given in weight percent.

Table 3.

Microprobe analyses of rinkite and nacareniobsite-(Ce) in naujaite pegmatite, marginal pegmatite, kakortokite and lujavrite

No.	1		2		3		4		5		6		7		8	
Rock	Nau.pegmatite		Nau.pegmatite		Nau.pegmatite		Marg. pegmatite		Kakortokite -6		Kakortokite +7		Lujavrite		Lujavrite	
Sample	104013		104013		104013		104358		104024		104016		104010		104010	
Mineral	Alteration		Nacareniobsite-(Ce)		Nacareniobsite-(Ce)		Rinkite		Rinkite		Rinkite		Nacareniobsite-(Ce)		Nacareniobsite-(Ce)	
Zone			Intermediate		Rim											
N	2		2		6		3		3		13		4		3	
Oxides wt%																
SiO_2	28.40	(.08)	28.57	(.08)	27.98	(.04)	29.07	(.07)	28.66	(.07)	29.55	(.03)	28.30	(.06)	28.50	(.07)
TiO_2	6.01	(.06)	4.03	(.05)	1.32	(.02)	6.87	(.05)	7.12	(.05)	5.86	(.02)	3.29	(.03)	1.50	(.03)
ZrO_2	0.37	(.06)	0.38	(.07)	0.12	(.01)	1.63	(.23)	0.78	(.11)	0.57	(.04)	0.12	(.02)	0.43	(.06)
Nb_2O_5	8.92	(.23)	10.22	(.24)	14.31	(.16)	3.04	(.12)	4.23	(.14)	6.11	(.07)	10.66	(.18)	13.77	(.23)
FeO	n.d.		n.d.		n.d.		n.d.		0.06	(.01)	0.03	(.00)	n.d.		n.d.	
CaO	18.80	(.09)	20.96	(.10)	18.30	(.06)	20.43	(.08)	23.03	(.08)	22.62	(.04)	19.72	(.07)	19.06	(.08)
Na_2O	2.97	(.09)	10.08	(.10)	11.18	(.06)	8.15	(.07)	7.90	(.07)	8.76	(.03)	9.95	(.07)	10.93	(.09)
La_2O_3	5.48	(.10)	4.80	(.09)	3.47	(.05)	2.93	(.06)	3.51	(.04)	3.53	(.03)	4.83	(.08)	4.34	(.07)
Ce_2O_3	11.40	(.12)	10.79	(.11)	11.47	(.07)	8.82	(.09)	10.10	(.10)	10.02	(.04)	11.25	(.08)	11.44	(.10)
Pr_2O_3	1.07	(.14)	1.16	(.14)	1.35	(.08)	1.22	(.12)	1.00	(.12)	1.14	(.05)	1.14	(.10)	1.19	(.12)
Nd_2O_3	3.71	(.17)	4.04	(.17)	5.45	(.10)	4.99	(.15)	4.99	(.15)	4.89	(.07)	4.04	(.12)	4.91	(.15)
Sm_2O_3	0.54	(.08)	0.55	(.08)	0.60	(.04)	0.83	(.06)	0.78	(.05)	0.77	(.04)	0.64	(.05)	0.55	(.07)
Y_2O_3	1.63	(.07)	1.07	(0.6)	0.49	(.03)	3.08	(.05)	1.69	(.06)	1.42	(.03)	0.95	(.06)	0.67	(.06)
F	4.46	(.24)	6.76	(.38)	6.29	(.19)	8.13	(.35)	6.74	(.30)	7.23	(.14)	6.21	(.23)	6.66	(.30)
Total	93.76		103.41		102.33		99.19		100.59		102.50		101.10		103.95	
-O for F	-1.88		-2.85		-2.65		-3.42		-2.84		-3.04		-2.61		-2.80	
	91.88		100.56		99.68		95.77		97.75		99.46		98.49		101.15	
Cations based on 4 Si																
Si	4.00		4.00		4.00		4.00		4.00		4.00		4.00		4.00	
Ti	0.64		0.42		0.14		0.71		0.75		0.60		0.35		0.16	
Zr	0.03		0.03		0.01		0.11		0.05		0.04		0.01		0.03	
Nb	0.57		0.65		0.92		0.19		0.27		0.37		0.68		0.87	
Fe	n.d.		n.d.		n.d.		n.d.		0.01		0.00		n.d.		n.d.	
Ca	2.84		3.14		2.80		3.01		3.44		3.28		2.99		2.87	
Na	0.81		2.73		3.09		2.17		2.13		2.30		2.72		2.97	
La	0.28		0.25		0.18		0.15		0.18		0.18		0.25		0.22	
Ce	0.59		0.55		0.60		0.44		0.52		0.50		0.58		0.59	
Pr	0.06		0.06		0.07		0.06		0.05		0.06		0.06		0.06	
Nd	0.19		0.20		0.28		0.25		0.25		0.24		0.20		0.25	
Sm	0.03		0.03		0.03		0.04		0.04		0.04		0.03		0.03	
Y	0.12		0.08		0.04		0.22		0.13		0.10		0.07		0.05	
F	1.98		2.99		2.84		3.54		2.97		3.10		2.78		2.96	
Cations	10.16		12.14		12.16		11.35		11.82		11.71		11.94		12.10	
Charges	31.83		33.57		33.49		31.90		33.09		32.63		33.11		33.42	

N: number of analyses. n.d.: not detected. Numbers in parentheses are standard deviations calculated on the basis of the total counting time and count rates on peak and background and given in weight percent.

value 12.00. The calculated F content is 2.96 apfu and the number of positive charges is 32.81.

The rosenbuschite group minerals are generally Zr-bearing. The mean value for Zr in the hainite from Ilímaussaq is 2.9 wt.% ZrO_2, which is low compared to hainite and götzenite from other localities (Cundari & Ferguson 1991; Sharygin *et al.* 1996; Johan & Cech 1989; Christiansen *et al.* 2003). The Ti+Nb content is 0.90 apfu (atoms per formula unit) and the apparent deficit, 0.10 apfu, is compensated by 0.08 Fe apfu and 0.02 Zr apfu. Most of the Zr, 0.16 apfu, is assigned to the M(1) site.

The Ilímaussaq hainite is rich in REE, 0.55 apfu, compared to götzenite and hainite from most localities (Sahama & Hytönen 1957; Cundari & Ferguson 1991; Sharygin *et al.* 1996; Christiansen *et al.* 2003; Johan & Cech 1989; Atencio *et al.* 1999), and only hainite from Langesund (Christiansen *et al.* 2003) has a comparable REE content, 0.44 apfu. It is notable that Y is the dominant REE in the hainite from Ilímaussaq. The crystal chemical formula for the average hainite from the pulaskite pegmatite is: $(Ca_{1.62}Zr_{0.16}Y_{0.22})(Na_{0.87}Ca_{1.11})(Ca_{1.65}REE_{0.35})Na(Ti_{0.81}Nb_{0.09}Fe_{0.08}Zr_{0.02})(Si_2O_7)_2O_{0.99}F_{2.96}$.

Backscattered electron images and microprobe analyses of sample 104029 revealed mineral grains enriched in REE compared to hainite (Fig. 2A). The interface towards hainite is sharp, without any sign of resorption, and parallel to one of the traces of the cleavages observed in hainite. These grains have a composition like rinkite (Table 2 no. 2). Compared to hainite, the contents of Ti, Nb and REE are higher and the Zr and Fe contents are lower, while the Y/(La+Ce) ratio is 0.74 compared to 1.10 in hainite. The REE patterns for hainite and two rinkite grains are given in Fig. 3A.

In thin section it is seen that hainite is altered to a brown and black material which in a backscattered electron image appears to be a fine-grained intergrowth of more than one phase (Fig. 2B). The mean composition is given in Table 2 no. 3.

Sodalite foyaite

The sodalite foyaite is characterised by a foyaitic texture formed by platy crystals of alkali feldspar up to 3 cm long, with interstitial nepheline, sodalite, Na-clinopyroxene, Na-amphibole and aenigmatite. Rinkite is an accessory mineral occurring as prismatic grains varying in size from micron scale to a few millimetres long. The crystals are often in parallel intergrowth with clinopyroxene and appear to have formed interstitially at a late stage in the crystallisation of the sodalite foyaite. Aggregates of prismatic rinkite are also embedded in analcime.

Two samples from the uppermost part of the sodalite foyaite (104374 and 104375) and a lower sample from just above the underlying naujaite (154346) have been analysed. All rinkite crystals are zoned with the lowest Nb content in the central part of the crystal. The highest Nb content, 7.4 wt.% Nb_2O_5, 0.46 Nb apfu, is found in the sample close to the naujaite. A backscattered electron image of rinkite in sample 104375 is shown in Fig. 2C. In the core of this crystal, Ti+Nb add up to 0.83 apfu (Table 2 no. 4), whereas they add up to 0.92 apfu in the mantle of the crystal (Table 2 no. 5) and 0.94 apfu in the narrow rim (Table 2 no. 6). The Zr content is normally less than 0.7 wt% ZrO_2, but the core of the zoned crystal has 2.2 wt% ZrO_2. Such a Zr enrichment in rinkite is only observed in this sample. The analysed rinkite crystals in samples 104374 and 154346 have Ti+Nb contents between 0.94 and 1.01 apfu.

Cerium is the dominant REE in the rinkite. In the Zr-enriched core the total REE content is 0.86 apfu (Table 2 no. 4). In other parts of this crystal the REE contents vary between 0.97 and 1.08 apfu (Table 2 nos 5 and 6).

The REE patterns for different parts of zoned rinkite crystals in sample 104375 and 154346 are shown in Figs 3B and 3C. The shapes of the REE patterns for the core, mantle and rim of the zoned crystal in sample 104375 are rather similar in the LREE region, whereas a slight Y decrease takes place from the core to the rim (Fig. 3B). For rinkite in sample 154346 the REE pattern for the core is similar to those in Fig. 3B whereas the REE pattern for the rim shows a distinct LREE enrichment (Fig. 3C).

Naujaite

Naujaite was examined in samples from three localities in the complex. All are typical naujaite with more or less densely packed euhedral crystals of sodalite up to about 0.5 cm across. Sodalite can make up more than 50 vol.% of some rocks. Microcline perthite forms laths up to several centimetres long which poikilitically enclose numerous sodalite crystals. Aegirine is the predominant mafic mineral and occurs as large poikilitic grains. Arfvedsonite occurs as parallel intergrowths in aegirine but may also form poikilitic grains. When rinkite is present it forms prismatic crystals from few millimetres up to more than 1 cm long. Rinkite grows in parallel alignment with aegirine and arfvedsonite in analcime–natrolite aggregates.

Rinkite crystals from the investigated naujaite samples (104001, 104034 and 104038) are slightly zoned, with 5.4–6.0 wt% TiO_2 and 6.0–7.6 wt% Nb_2O_5. The Zr variation is 0.3–1.2 wt% ZrO_2. One analysis (sample 104001) is listed in Table 2 no. 7. The REE patterns for two slightly different parts of this crystal are shown in Fig. 3D.

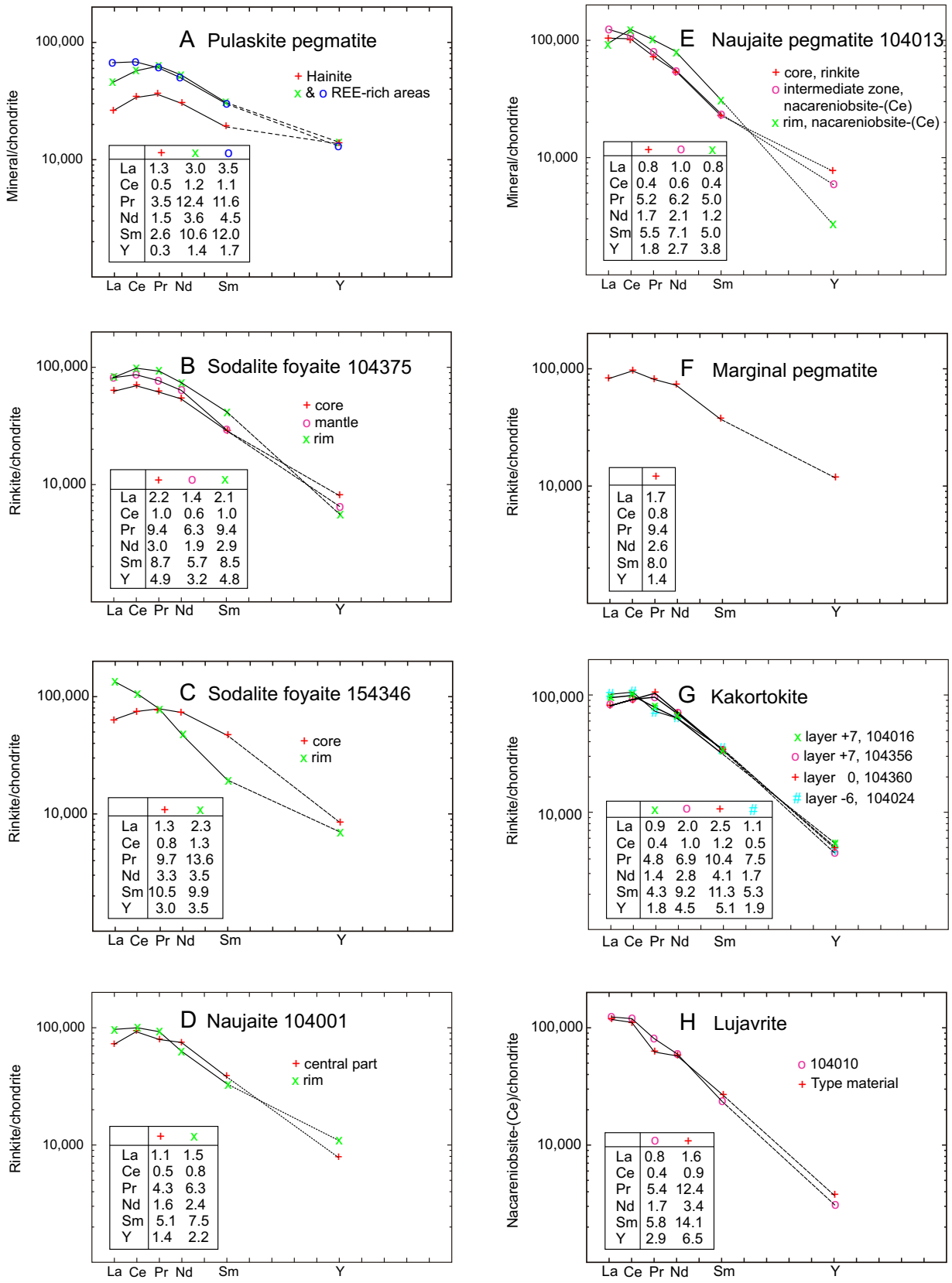

Fig. 3. Chondrite-normalised REE patterns for hainite, rinkite and nacareniobsite-(Ce) in different Ilímaussaq rocks. Chondrite normalisation factors from Boynton (1983). The standard deviations, listed in each diagram, are calculated on the basis of the total counting time and count rates on peak and background and given in per cent.

Naujaite pegmatite

The pegmatitic facies of naujaite (sample 104013) is generally rich in sodalite. Prismatic aegirine may grow between the sodalite crystals to form a poikilitic texture, and aegerine crystals often enclose arfvedsonite in parallel growth. Zoned rinkite–nacareniobsite-(Ce) grains occur in some pegmatites as prismatic crystals that may attain lengths of several centimetres and in places poikilitically enclose sodalite. Rinkite–nacareniobsite-(Ce) grains are often altered into a brownish material. Backscattered electron images show that the crystals are zoned, and often three zones with different Ti and Nb contents can be identified (Fig. 2D). Interlobal borders between the different zones indicate partial resorption prior to the formation of the next zone (Figs 2D and 2E).

The central and dominating parts of the crystals have 5.4–4.3 wt% TiO_2 and 7.1–9.4 wt% Nb_2O_5 and represent intermediate members of the rinkite–nacareniobsite-(Ce) solid solution series (Table 2 nos 8 and 9). The outer parts of the cores are often altered (Figs 2D–F) and show a marked Na and Ca leaching (Table 3 no. 1). The intermediate zones are less developed; when present they have 3.5–4.0 wt% TiO_2 and 9.8–10.9 wt% Nb_2O_5 (Table 3 no. 2). In the rim zones the Ti content is reduced to approximately 1.3 wt% TiO_2 whereas the Nb content is more than 14.0 wt% Nb_2O_5 (Table 3 no. 3).

The REE patterns for different zones in rinkite–nacareniobsite-(Ce) crystals in a naujaite pegmatite are shown in Fig. 3E. The three REE patterns represent mean values for rims, intermediate zones and cores. The rim zones have lower La and Y compared to the cores, whereas the intermediate zones show a slight La enrichment compared to the cores.

Marginal pegmatite

The marginal pegmatite occurs along the contact between the kakortokite and the country rock. The zone is characterised by its heterogeneity and consist of a matrix of massive kakortokite-like rocks cut by an anastomosing network of pegmatite veins. The thickness decreases upwards from about 100 m to 25 m (Bohse & Andersen 1981). At the south coast of Kangerluarsuk the pegmatite passes gradually laterally into the kakortokite. The matrix in the marginal pegmatite is supposed to be the border facies for the lower part of the complex, the kakortokites and lujavrites (Bohse & Andersen 1981; Sørensen 2006).

The pegmatite veins consist of crystals of eudialyte, sodalite, nepheline, perthitic alkali feldspar, albite and aegirine in a matrix of analcime, natrolite and tugtupite. Scattered grains of aenigmatite are partly overgrown with ussingite. Rinkite occurs as prismatic grains in natrolite and grows along the large crystals of aegirine. Rinkite prisms also form sheath-like aggregates. The examined sample (104358) is from the uppermost part of Laksetværelv close to the contact against the augite syenite.

The investigated crystals show only minor compositional variation, with 6.8–7.0 wt% TiO_2. The Zr and Y contents are slightly elevated, 1.6 wt% ZrO_2 and 3.1 wt% Y_2O_3, compared to most other rinkites. The analyses are characterized by low totals with a mean value of 95.77, indicating minor alteration although it was not observed during the analytical work. The Ti+Nb sum is 0.90 apfu whereas the Ti+Nb+Zr sum is 1.01 apfu (Table 3 no. 4). The REE pattern is given in Fig. 3F.

Kakortokite

The major part of the kakortokite is layered. A total of 29 unit are exposed and numbered from –11 to +17 (Bohse & Andersen 1981). Rinkite is a rare component and occurs as small prismatic grains up to 5 mm long, interstitial to laths of microcline. Rinkite may also grow along or across grains of aegirine and be associated with eudialyte. Sørensen & Larsen (1987) pointed out that the amount of rinkite appears to increase upwards in each unit.

The investigated rinkite material includes samples from unit –6 (104024), unit 0 (104360), and unit +7 (104016 and 104356). The TiO_2 content varies between 7.1 and 5.4 wt% TiO_2 (Table 3 nos 5 and 6), and the data suggest Nb enrichment in the rinkite upwards in the layered succession, from about 4 to about 6 wt% Nb_2O_5. The REE patterns for rinkite from units – 6, 0 and +7 are given in Fig. 3G. There is no significant stratigraphic evolution in REE.

Lujavrite and late veins

Two nacareniobsite-(Ce) bearing samples were examined. One of them (104010) is from the northern branch of Lilleelv at the head of Kangerluarsuk. It is a dyke of black arfvedsonite lujavrite intersecting naujaite pegmatite. The extremely fine-grained rock is faintly layered. It contains thin prismatic or ruler-shaped grains, up to 5 cm long, of nacareniobsite-(Ce). In thin section the rock is seen to be composed of stout prismatic grains of arfvedsonite which make up about 50 vol.%, albite laths, eudialyte, nepheline and rounded grains of sodalite and analcime. The prismatic grains of nacareniobsite-(Ce) are zoned and enclose needles of arfvedsonite and aegirine. The investigation also includes the type material from Kvanefjeld (Petersen *et al.* 1989). At this locality nacareniobsite-(Ce) occurs in dissolution cavities in black arfvedsonite lujavrite. The

mineral is clearly of late- and post-magmatic origin, in accordance with its presence in late ussingite veins.

In the zoned nacareniobsite-(Ce) grains in sample 104010 the Nb content varies between 10.7 and 13.8 wt% Nb_2O_5. Selected analyses are listed in Table 3 nos 7 and 8. The REE patterns for nacareniobsite-(Ce) from the two different localities are very similar (Fig. 3H).

Discussion

The rinkite–nacareniobsite-(Ce) solid solution series

Structural data (Galli & Alberti 1971; Sokolova & Hawthorne 2008; Cámara *et al.* 2011) confirm that rinkite and nacareniobsite-(Ce) are isostructural and have the ideal formulae $Na_2Ca_4REETi(Si_2O_7)_2OF_3$ and $Na_3Ca_3REENb(Si_2O_7)_2OF_3$, as suggested by Petersen *et al.* (1989). The structural determinations assign the REE to two different sites, M(1) and M(3), which also contain Ca. However, the rinkite data from different localities presented by Cámara *et al.* (2011) show some divergence from the ideal composition. In rinkite from Mont Saint-Hilaire the REE content is only 0.75 apfu. In our samples we have observed comparably low REE contents in the material found intergrown with hainite (Table 2 no. 2) and in the cores of zoned grains in the sodalite foyaite (Table 2 no. 4). We assume that these crystals are rinkite.

The structural data assign Ti and Nb to the M(5) site together with minor amounts of Zr and Ta (Galli & Alberti 1971; Sokolova & Hawthorne 2008; Cámara *et al.* 2011). The formula calculations of our microprobe analyses normally have Ti+Nb close to the ideal value of 1.0, and when the sum is 0.90 apfu or lower the deficit is compensated by increased Zr as seen in the rinkite from the sodalite foyaite (Table 2 no. 4) and the marginal pegmatite (Table 3 no. 4).

The Nb versus Ti+Zr diagram in Fig. 4 shows a strong negative correlation (slope: -1.04, r: -0.989), confirming the $Ti^{4+} = Nb^{5+}$ substitution in the M(5) site of the rinkite–nacareniobsite-(Ce) series. The diagram further shows that the rinkite–nacareniobsite-(Ce) compositions in the Ilímaussaq complex span almost the full extension of the solid solution series and confirm its continuity. Moreover, the roof sequence and the floor sequence show similar compositional evolution, with the most Ti-rich compositions in the less evolved rocks (pulaskite pegmatite and marginal pegmatite) and the most Nb-rich compositions in the most evolved rocks (naujaite pegmatite and lujavrite).

The REE contents show a considerable variation, from 0.83 apfu in rinkite in pulaskite pegmatite to 1.31 apfu in nacareniobsite-(Ce) from naujaite pegmatite. The relation between REE and Nb in the solid solution series is shown in Fig. 5. In rinkite from the roof sequence there is a 1:1 correlation (slope: 1.0, r: 0.94) between REE and Nb content, whereas rinkite from the marginal pegmatite and kakortokite unit –6 differ significant from this trend with a REE content of about 1.15 apfu. In the nacareniobsite-(Ce) part of the solid solution series the correlation between REE and Nb is less pronounced and different (slope: 0.43, r: 0.68). If the rinkite analyses from the less

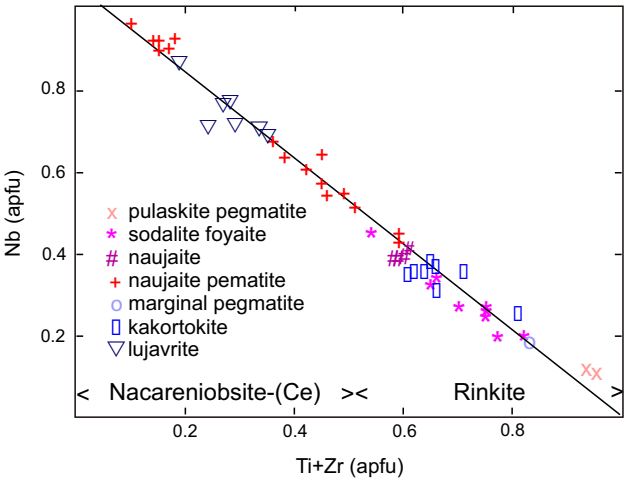

Fig. 4. Ti+Zr versus Nb in the rinkite–nacareniobsite-(Ce) solid solution series in Ilímaussaq. The solid line represents the regression line; slope: -1.04, r: -0.99.

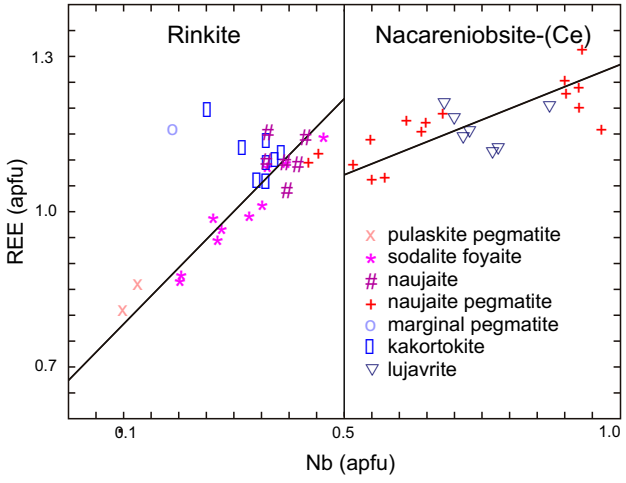

Fig. 5. Nb versus REE in the rinkite–nacareniobsite-(Ce) solid solution series in Ilímaussaq. The solid lines represent regression lines. Rinkite analyses in pulaskite pegmatite, sodalite foyaite and naujaite; slope: 1.0, r: 0.94. Nacareniobsite-(Ce) analyses in naujaite and lujavrite; slope: 0.58, r: 0.68.

evolved roof rocks, pulaskite and sodalite foyaite, are excluded from the comparison, it may be argued that the REE contents in the rinkite-nacareniobsite-(Ce) solid solution are almost independent of the Nb content (Fig. 5).

Petersen *et al.* (1989) suggested that the increase in Nb from rinkite to nacareniobsite-(Ce) is stoichiometrically balanced by the coupled substitution $Ti^{4+} + Ca^{2+} = Nb^{5+} + Na^{+}$. However the concurrent increase in the REE content in rinkite from the roof sequence should also be charge compensated. For REE as well as Nb this could be achieved by the above-mentioned substitution and the coupled substitution $2Ca^{2+} = Na^{+} + REE^{3+}$, but also through a $F^{1-} = O^{2-}$ substitution in the X site.

The idealized F content in the rinkite–nacareniobsite-(Ce) series is 3.0 apfu according to the proposed formulae in the literature. However, we found higher F contents than this. In rinkite with Nb<0.33 apfu the F content is 3.23 ± 0.22 apfu, whereas the F content is 2.84 ± 0.26 apfu in nacareniobsite-(Ce) with Nb>0.75 apfu. Our data therefore indicate some $F^{1-} = O^{2-}$ substitution in the X site; however, the Na versus REE+Nb plot in Fig. 6 (slope: 0.936, r: 0.976) shows that the Nb and REE enrichment in both minerals is primarily compensated by the $Ca^{2+} = Na^{+}$ substitution. This compensation model was also suggested by Cámara *et al.* (2011).

Hainite and götzenite

Besides the major cations in hainite and götzenite: Na, Ca, Ti and Si, the two minerals contain Zr and REE in various amounts. A reinvestigation of the hainite type material by Johan & Cech (1989) documented

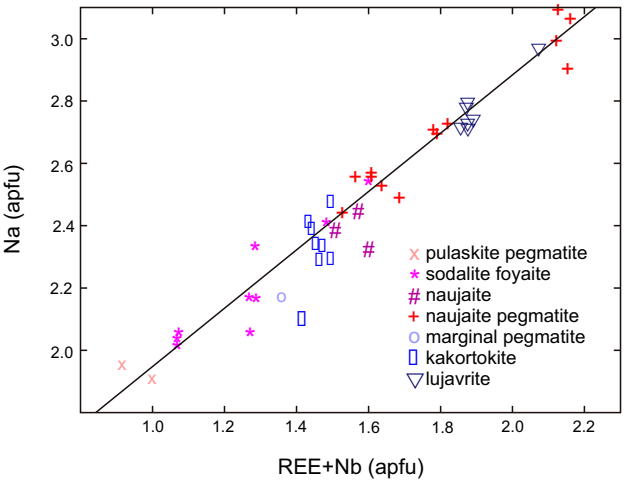

Fig. 6. Na versus REE+Nb in the rinkite–nacareniobsite-(Ce) solid solution series in Ilímaussaq. The solid line represents the regression line; slope: 0.936, r: 0.98.

the presence of 6.5 wt% ZrO_2 and minor amounts of REE. Christiansen *et al.* (2003) reported 1.4 wt% ZrO_2 and 6.1 wt% REE_2O_3 in götzenite from Langesund and 4.0 wt% ZrO_2 and 9.9 wt% REE_2O_3 in hainite from Werner Bjerge, East Greenland. Lower concentrations of Zr and REE are reported in götzenite from Pian di Celle Volcano by Sharygin *et al.* (1996) and Bellezza *et al.* (2004), and in hainite from Pocos de Caldas by Atencio *et al.* (1999). The crystal structural data for the two minerals show that Zr, Y and other REE are concentrated in the M(1) site, whereas only a minor amount of REE is located in the M(3) site.

Sharygin *et al.* (1996) suggested that the substitution $Ca^{2+} + 2F^{1-} = Zr^{4+} + 2O^{2-}$ played a major role in götzenite from Pian di Celli. However, the REE and Zr substitutions for Ca in the M(1) and M(3) sites and Nb for Ti in the M(5) site in götzenite and hainite could in principle also be stoichiometrically balanced by substitutions such as $2Ca^{2+} = REE^{3+} + Na^{+}$, $3Ca^{2+} = Zr^{4+} + 2Na^{+}$ and $Ca^{2+} + Ti^{4+} = Na^{+} + Nb^{5+}$ as observed for the rinkite–nacareniobsite-(Ce) series.

The published microprobe analyses of götzenite and hainite show that most samples contain Zr, Y and REE; however one of the götzenite analysis from Pian di Celli (Sharygin *et al.*; 1996) approach the ideal end member $NaCa_6Ti(Si_2O_7)_2OF_3$, whereas no hainite analysis is near to the Zr, Y and REE free ideal end member, $Na_2Ca_5Ti(Si_2O_7)_2(OH)_2F_2$, suggested by Atencio *et al.* (1999).

For comparison with our data we have calculated the cation contents of 20 published hainite and götzenite analyses on the basis of 4 Si atoms. The calculated mean number of cations for the published analyses is 12.0 ± 0.1 for hainite and 11.8 ± 0.2 for götzenite, the ideal being 12.0. The mean number of positive charges is calculated to be 32.9 ± 0.2 for hainite and 32.8 ± 0.2 for götzenite. However, some examples such as hainite from Hradiste (Johan & Cech 1989) have a low cation content (11.7) and a low number of positive charges. The calculated Ca and Na contents in the published hainite and götzenite analyses are plotted in Fig. 7. This shows that there is a good negative correlation between the two elements (slope: -0.58 r: -0.98), indicating that only approximately half of the Ca atoms are replaced by Na. The published data do not indicate the existence of the hainite end member suggested by Atencio *et al.* (1999), but a compositional variation between 'end members' having $NaCa_6$ and Na_2Ca_4 in the M(1)–M(4) sites, which suggests that one Ca cation should be replaced by REE, Y and/or Zr.

The charge balancing mechanism for the Y, REE and Zr substitution in the M(1) –M(4) sites and Nb for Ti in M(5) can be further evaluated by comparing the calculated Na apfu content and the excess of positive charges (EPC) introduced by the above-mentioned substitu-

tion, using the equation EPC = REE + Y + 2*Zr(M(1)) + Nb –2*Fe^{2+}(M(5)). The plot (Fig. 8) shows that there is a high positive correlation (slope: 0.91, r: 0.98) between Na and EPC, indicating that the increase in Na from 1.0 to 1.9 apfu is primarily related to the introduction of REE, Y, Zr and Nb by the charge compensating substitutions $2Ca^{2+} = REE^{3+} + Na^{+}$, $3Ca^{2+} = Zr^{4+} + 2Na^{+}$ and $Ca^{2+} + Ti^{4+} = Na^{+} + Nb^{5+}$, whereas the substitution $Ca^{2+} + 2F^{1-} = Zr^{4+} + 2O^{2-}$ can only play a minor role. The previously published analyses and our data thus indicate that the investigated götzenite–hainite samples show a compositional variation between the following ideal end members: $NaCa_6Ti(Si_2O_7)_2OF_3$ and $(Y,REE,Zr)Na_2Ca_4Ti(Si_2O_7)_2OF_3$. The content of F in the X-position in hainite and götzenite has been discussed by Sokolova (2006) who concluded that the chemical formulae for hainite and götzenite should be based on OF_3, in contradiction to the formula given by Rastsvetaeva *et al.* (1995), Atencio *et al.* (1999) and Christiansen *et al.* (2003).

REE evolution in investigated minerals related to the evolution of the Ilímaussaq complex

In hainite and the rinkite–nacareniobsite-(Ce) series the REE are located in the M(1) and M(3) sites. In rinkite–nacareniobsite-(Ce) the average bond lengths for the two sites deviate by less than 1% (Sokolova & Hawthorne 2008; Cámara *et al.* 2011), whereas the differences between the two sites can be more than 4% in hainite–götzenite (Christiansen *et al.* 2003), favouring the Zr, Y and HREE substitution for Ca in the M(1) site in hainite–götzenite. These crystal structural differences can explain the relatively high Y content in the Ilímaussaq hainite but also mean that a comparison of the REE patterns for hainite with the patterns for rinkite–nacareniobsite-(Ce) is not meaningful.

The chondrite normalised REE patterns for rinkite–nacareniobsite-(Ce) from the roof sequence in Fig. 3A–E and the floor sequence in Fig. 3F–H show identical changes with evolution of the magmas. During the evolution of both sequences there is a slight relative increase in La and Ce and a relative decrease in Y from rinkite in pulaskite pegmatite and marginal pegmatite to nacareniobsite-(Ce) in naujaite pegmatite and lujavrite. A comparable evolution was observed for REE in apatite from the roof sequence (Rønsbo 2008). Relatively similar REE patterns are observed in rinkite from the less evolved rocks: pulaskite pegmatite, sodalite foyaite and marginal pegmatite; also the more evolved naujaite and kakortokite have similar REE patterns, and so have nacareniobsite-(Ce) in the most evolved rocks naujaite pegmatite and lujavrite. These data support the conclusion that the REE content in the roof and floor sequences evolved in a similar way (Rønsbo 2008).

Conclusions

Rinkite is a minor mineral in the Ilímaussaq complex. In the roof sequence it occurs in all investigated rock types (pulaskite pegmatite, sodalite foyaite, naujaite and naujaite pegmatite); in the floor sequence it occurs in marginal pegmatite and kakortokite but not in lujavrite. In pulaskite pegmatite it is intergrown with hainite. Nacareniobsite-(Ce) occurs in the most evolved rocks in both the roof and floor sequences, respectively in naujaite pegmatite and lujavrite, as

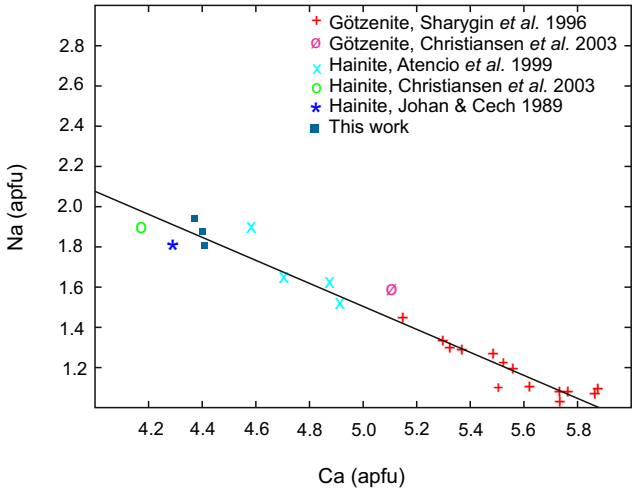

Fig. 7. Na versus Ca in hainite and götzenite in published and present analyses. The solid line represents the regression line; slope: -0.58, r: -0.98.

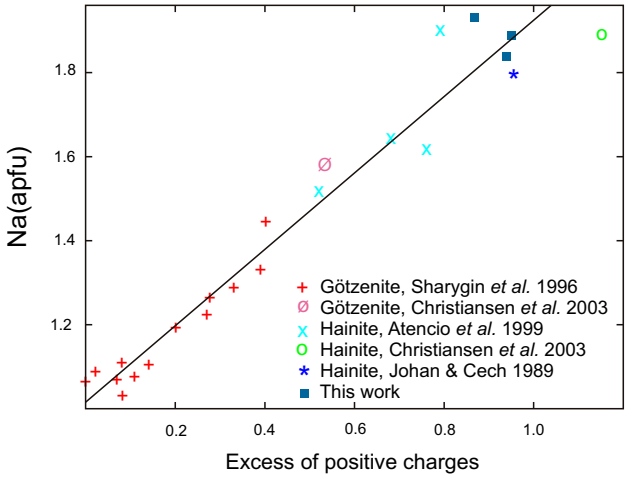

Fig. 8. Na versus Excess of positive charges (EPS) in hainite and götzenite in published and present analyses. The solid line represents the regression line; slope: 0.91, r: 0.98.

overgrowths on rinkite in naujaite pegmatite and as individual crystals in both rock types. The two minerals are members of a solid solution series, and in both the roof sequence and the floor sequence the compositional variation spans from rinkite in the less evolved rocks to nacareniobsite-(Ce) in the most evolved rocks.

Rinkite crystals in sodalite foyaite and naujaite pegmatite have developed a pronounced zonation, and three generations can be observed. Particularly crystals from the naujaite pegmatite represent intermediate members of the rinkite–nacareniobsite solid solution series.

Rinkite in the roof sequence shows an increase in REE contents from 0.83 apfu in Nb-poor rinkite in pulaskite pegmatite to 1.15 apfu in Nb-rich rinkite from sodalite foyaite and naujaite. In the floor sequence, rinkite in marginal pegmatite and kakortokite has REE contents around 1.15 apfu without a specific trend. In the nacareniobsite-(Ce) part of the solid solution series there is also an increase in the REE content with increasing Nb content, but less pronounced.

The chondrite normalised REE patterns for rinkite–nacareniobsite-(Ce) from the roof and floor sequences show identical changes with evolution. In both sequences there is a slight relative increase in La and Ce, and a relative decrease in Y, from rinkite in pulaskite pegmatite and marginal pegmatite to nacareniobsite-(Ce) in naujaite pegmatite and lujavrite. Further, rinkite in the less evolved rocks (pulaskite pegmatite, sodalite foyaite and marginal pegmatite) show mutually similar REE patterns; rinkite in the more evolved rocks (naujaite and kakortokite) show mutually similar REE patterns; and nacareniobsite-Ce in the most evolved rocks (naujaite pegmatite and lujavrite) also show mutually similar REE patterns.

The REE and Nb in the rinkite–nacareniobsite-(Ce) series are primarily stoichiometrically balanced by the coupled substitutions $2Ca^{2+} = Na^{+} + REE^{3+}$ and $Ti^{4+} + Ca^{2+} = Nb^{5+} + Na^{+}$.

The presence of hainite in a pulaskite pegmatite is established by X-ray powder diffraction data and single crystal information coupled with microprobe analysis. The mineral has a high REE content compared to published hainite and götzenite analyses and has Y as the dominant REE. The empirical formula is $(Ca_{1.62}Zr_{0.16}Y_{0.22})(Na_{0.87}Ca_{1.11})(Ca_{1.65}REE_{0.35})Na(Ti_{0.81}Nb_{0.09}Fe_{0.08}Zr_{0.02})(Si_2O_7)_2O_{0.99}F_{2.96}$, calculated on the basis of the microprobe analyses.

Based on previously published analyses it is suggested that the götzenite–hainite solid solution series shows compositional variation between the ideal end members $NaCa_6Ti(Si_2O_7)_2OF_3$ and (Y,REE,Zr) $Na_2Ca_4Ti(Si_2O_7)_2OF_3$.

Acknowledgements

We thank Eugene I. Semenov for the hainite sample and Henrik Friis and Helene Almind for the single crystal investigation. We further thank John C. Bailey, Lotte M. Larsen and the reviewers Tonci Balic-Zunic and Adrian Finch for valuable criticism. The field work in the Ilímaussaq alkaline complex was partly supported by INTAS project no. 93–1474.

References

Andersen, S., Bohse, H. & Steenfelt, A. 1981: A geological section through the southern part of the Ilímaussaq intrusion. Rapport Grønlands Geologiske Undersøgelse 103, 39–42.

Atencio, D., Coutinho, J.M.V., Ulbricht, M.N.C., Vlach, S.R.F., Rastsvetaeva, R.K. & Pushcharovskii, D.Y. 1999: Hainite from Pocos de Caldas, Minas Gerais, Brazil. Canadian Mineralogist 37, 91–98.

Bailey, J.C., Gwozdz, R., Rose-Hansen, J. & Sørensen, H. 2001: Geochemical overview of the Ilímaussaq alkaline complex, South Greenland. Geology of Greenland Survey Bulletin 190, 35–53.

Bellezza, M., Merlino, S. & Perchiazzi, N. 2004: Chemical and structural study of the Zr-, Ti-disilicates in the venanzite from Pian di Celle, Umbria, Italy. European Journal of Mineralogy 16, 957–969.

Bellezza, M., Merlino, S., Perchiazzi, N. & Raade, G. 2009a: "Johnstrupite" : A chemical and structural study. Atti della Societá Toscana di Scienza Naturali, Serie A 114, 1–3.

Bellezza, M., Merlino, S. & Perchiazzi, N. 2009b: Mosandrite: structural and crystal-chemical relationships with rinkite. Canadian Mineralogist 47, 897– 908.

Blumrich, J. 1893: Die Phonolite des Friedländer Bezirkes in Nordböhmen. Tschermaks Mineralogische und Petrographische Mitteilungen 13, 465–495.

Bohnsted, E.M. 1926: Two new minerals of the mosandrite group from Khibina Tundra. Bulletin of the Academy of Sciences of USSR 20, 1181 (in Russian).

Bohse, H. & Andersen, S. 1981: Review of the stratigraphic divisions of the kakortokite and lujavrite in southern Ilímaussaq. Rapport Grønlands Geologiske Undersøgelse 103, 53–62.

Boynton, W.V. 1983: Cosmochemistry of rare earth elements: meteoritic studies. In: Henderson, P. (ed): Rare Earth Element Geochemistry, 63–114. Amsterdam: Elsevier.

Brøgger, W.C. 1890: Die Mineralien der Syenitpegmatitgänge der südnorwegischen Augit- Nephelinsyenite. Zeitschrift für Kristallographie 16, 586–597.

Cámara, F., Sokolova, E. & Hawthorne, F.C. 2011: From structural topology to chemical composition. XII. Titanium silicates: the crystal chemistry of rinkite $Na_2Ca_4REETi(Si_2O_7)_2OF_3$. Mineralogical Magazine 75, 2755–2774.

Canillo, E., Mazzi, F. & Rossi, G. 1972: Crystal structure of götzenite. Soviet Physics and Crystallography 16, 1026–1030.

Christiansen, C.C., Johnsen, O. & Makovicky, E. 2003: Crystal chemistry of the rosenbuschite group. Canadian Mineralogist 41, 1203–1224.

Cundari, A. & Ferguson, A.K. 1991: Petrogenetic relationships between melilitite and lamproite. Contributions to Mineralogy and Petrology 107, 343–357.

Erdmann, A 1841: Mosandrite. In: J.J. Berzelius. Jahresbericht über die Fortschritte der physischen Wissenschaften 21, 178–179.

Fleischer, M. 1958: Rinkite, johnstrupite, rinkolite, lovchorrite and calcium rinkite (all = mosandrite). American Mineralogist 43, 795–796.

Fleischer, M. 1987: Glossary of Mineral Species, 5th edition. Mineralogical Record Corporation. Tucson, Arizona, 227 pp.

Galli, E. & Alberti, A. 1971: The crystal structure of rinkite. Acta Crystallographica B27, 1277–1284.

Giester, G., Pertlik, F. & Ulrych, J. 2005: Die kristallstruktur des minerals hainite. Mitteilungen der Österreichischen Mineralogischen Geselschaft 151, p. 45.

Johan, Z. & Cech, F. 1989: Nouvelles données sur la haïnite, $Na_2Ca_4[(Ti, Zr, Mn, Fe Nb, Ta)_{1,5}\square_{0,5}](Si_2O_7)_2F_4$ et ses relations cristallochimiques avec götzenite, $Na_2Ca_5Ti(Si_2O_7)_2F_4$. Comptes Rendus de l'Académie des Sciences, Paris, 308, Série. II, 1237–1242.

Larsen, L.M. & Sørensen, H. 1987: The Ilímaussaq intrusion – progressive crystallisation and formation of layering in an agpaitic magma. In: Fitton, J.G. & Upton, B.G.J. (eds), Alkaline Igneous Rocks. Special Publication, Geological Society, London 30, 473–488.

Lorenzen, J. 1884: Untersuchungen einiger Mineralien aus Kangerdluarsuk in Grönland. Zeitschrift für Kristallographie 9, 243–254.

Marks, M. & Markl, G. 2001: Fractionation and assimilation processes in the alkaline augite syenite unit of the Ilímaussaq intrusion, South Greenland, as deduced from phase equilibria. Journal of Petrology 46, 1947–1969.

Petersen, O.V. 2001: List of all minerals in the Ilímaussaq alkaline complex, South Greenland. In Sørensen, H. (ed.): The Ilímaussaq alkaline complex, South Greenland: status of mineralogical research with new results. Geology of Greenland Survey Bulletin 190, 25–33.

Petersen, O.V., Rønsbo, J.G. & Leonardsen, E.S. 1989: Nacareniobsite-(Ce), a new mineral species from the Ilímaussaq alkaline complex, South Greenland, and its relation to mosandrite and the rinkite series. Neues Jahrbuch für Mineralogie Monatshefte 2, 84–96.

Rastsvetaeva, R.K., Pushcharovskii, D.Y. & Atenzio, D. 1995: Crystal structure of giannetite. Crystallography Reports 40, 574–578.

Rønsbo, J.G. 1989: Coupled substitution involving REEs and Na and Si in apatites in alkaline rocks from the Ilímaussaq intrusion, South Greenland, and the petrological implications. American Mineralogist 74, 896-901.

Rønsbo, J.G. 2008: Apatite in the Ilímaussaq alkaline complex: occurrence, zonation and compositional variation. Lithos 106, 71–82.

Sahama, T.G. & Hytönen, K. 1957: Götzenite and combeite, two new silicates from Belgian Congo. Mineralogical Magazine 31, 503–510.

Semenov, E.I. 1969: The mineralogy of the Ilímaussaq alkaline massif. Izvestiya Akademii Nauk SSSR, 412 pp. (in Russian).

Sharygin, V.V., Stoppa, F. & Kolesov, B.A. 1996: Zr-Ti disilicates from the Pian di Celle volcano, Umbria, Italy. European Journal of Mineralogy 8, 1199–1212.

Slepnev, Y.S. 1957: On minerals of the rinkite group. Izvestiya Akademii Nauk SSSR, Seriya geologicheskaya 3, 63–75. (in Russian).

Sokolova, E. 2006: From structure topology to chemical composition. I. Structural hierarchy and stereochemistry in titanium disilicate minerals. Canadian Mineralogist 44, 1273–1330.

Sokolova E. & Cámara F. 2008: From structural topology to chemical composition. VIII. Titanium silicates: the crystal chemistry of mosandrite from the type locality of Låven (Skådön), Langesundsfjorden, Larvik, Vestfold, Norway. Mineralogical Magazine 72, 887–897.

Sokolova, E. & Hawthorne, F.C. 2008: From structural topology to chemical composition. V. Titanium silicates: crystal chemistry of nacareniobsite-Ce. Canadian Mineralogist 46, 1323–1342.

Sørensen, H. 2006: The Ilímaussaq alkaline complex, South Greenland – an overview of 200 years of research and an outlook. Meddelelser om Grønland, Geoscience 45, 70 pp.

Sørensen H. & Larsen, L.M. 1987: Layering in the Ilímaussaq alkaline intrusion. In: Parsons, I. (ed.) Origins of Igneous Layering. NATO Advanced Science Institute Series C, Mathematical and Physical Sciences 196, 1–28. Dordrecht: D. Reidel Publishing Company.

Sørensen, H, Bailey, J.C. & Rose-Hansen, J. 2011: The emplacement and crystallization of the U-Th-REE-rich agpaitic and hyperagpaitic lujavrites at Kvanefjeld, Ilímaussaq alkaline complex, South Greenland.

Steenfelt, A. 1981: Field relations in the roof zone of the Ilímaussaq intrusion with special reference to the position of the alkali acid rocks. Rapport Grønlands Geologiske Undersøgelse 103, 43–52.

Upton, B.G.J. 2013: Tectono-magmatic evolution of the younger Gardar southern rift, South Greenland. Geological Survey of Denmark and Greenland, Bulletin 29, 124 pp.

Ussing, N.V. 1912: Geology of the country around Julianehaab, Greenland. Meddelelser om Grønland 38, 426 pp.